Environment International 135 (2020) 105356

Contents lists available at ScienceDirect

Environment International

journal homepage: www.elsevier.com/locate/envint

Potential applications of graphene-based nanomaterials as adsorbent for removal of volatile organic compounds

Vanish Kumar[a,1], Yoon-Seo Lee[b,1], Jae-Won Shin[b,1], Ki-Hyun Kim[b,*], Deepak Kukkar[c,*], Yiu Fai Tsang[d,*]

[a] National Agri-Food Biotechnology Institute (NABI), S.A.S. Nagar, Punjab 140306, India
[b] Department of Civil and Environmental Engineering, Hanyang University, 222 Wangsimni-ro, Seoul 04763, Republic of Korea
[c] Department of Nanotechnology, Sri Guru Granth Sahib World University, Fatehgarh Sahib, Punjab 140406, India
[d] Department of Science and Environmental Studies, The Education University of Hong Kong, Tai Po, New Territories, Hong Kong

ARTICLE INFO

Handling Editor: Da Chen

Keywords:
Graphene-based materials
VOCs
Adsorption
Adsorption mechanism
Partition coefficient

ABSTRACT

In recent years, graphene-based materials (GBMs) have been regarded as the core technology in diverse research fields. Consequently, the demand for large-scale synthesis of GBMs has been increasing continuously for various fields of industry. These materials have become a competitive adsorbent for the removal of environmental pollutants with improved adsorption capacity and cost effectiveness through hybridization or fabrication of various functionalities on their large surface. In particular, their applicability opens up new avenues for the adsorptive removal of volatile organic compounds (VOCs) (e.g., through the build-up of efficient air purification systems). This review explored the basic knowledge and synthesis approaches for GBMs and their performances as adsorbent for VOC removal. Moreover, the mechanisms associated with the VOC removal were explained in detail. The performance of GBMs has also been evaluated along with their present limitations and future perspectives.

1. Introduction

Air pollution is a serious issue in the developing world with rapid industrial development and population growth becasue of its destructive potential to deteriorate human health or environmental conditions (Brunekreef and Holgate 2002; Kampa and Castanas 2008; Mishra 2019). As the cause of acid rain and smog, the emission of diverse pollutants (e.g., volatile organic compounds (VOCs), nitrogen oxides (NO_x), and sulfur dioxide (SO_2)) into the atmosphere can pose health hazards with various environmental implications and social ramifications (e.g., losses in working time) (Likens and Bormann 1974; Likens et al., 1996; Monzón and Guerrero 2004; Szczęśniak et al., 2018a). Among a list of airborne polutants, the deleterious effects of VOCs are well-known to affect human life by causing diverse diseases (e.g., cancer, pharyngitis, nausea, headaches, and emphysema) and even death (Chu et al., 2018; Szczęśniak et al., 2018a). Therefore, the development of cost-effective purification technologies for VOCs has become the need of the hour to protect the atmospheric environment.

To date, a number of removal approaches have been employed to remove VOCs from the environment, e.g., adsorption (Cheng et al., 2019; Kumar et al., 2019; Veerapandian et al., 2019), condensation (Belaissaoui et al., 2016), catalytic oxidation (Kamal et al., 2016; Wang et al., 2017), biodegradation (Cheng et al., 2016; Li et al., 2013), incineration (Campesi et al., 2015; Chu et al., 2018), and thermal oxidation (Mao et al., 2015). Among these options, adsorption has been regarded as one of the most preferable choices for VOC abatement due to its high efficiency, easy operation, good accessibility, low cost, feasibility to implement at large scale, and ease of regeneration (Chu et al., 2018; Minitha et al., 2017). Conventional adsorbents such as activated carbon (AC) and polymers have been widely used in the treatment of pollutants due to their ease of implementation (Smith and Rodrigues 2015). However, the conventional adsorbents, especially AC are not sufficiently effective to treat certain types of target molecules (e.g., gaseous VOCs with low molecular weight like formaldehyde) (Hu et al., 2018; Kumar et al., 2019). The functionality required to capture such VOCs is unlikely to be present or insufficient in AC. Likewise, other systems such as filters (e.g., carbon filters) are not effective to treat polar VOCs, e.g., NH_3 and H_2S (DeCoste and Peterson 2014).

To overcome such limitations of conventional adsorbents, the demand for novel functional adsorbents developed from carbon-based

* Corresponding authors.
E-mail addresses: kkim61@hanyang.ac.kr (K.-H. Kim), dr.deepakkukkar@gmail.com (D. Kukkar), tsangyf@eduhk.hk (Y. Fai Tsang).
[1] Co-first author.

https://doi.org/10.1016/j.envint.2019.105356
Received 2 September 2019; Received in revised form 15 November 2019; Accepted 20 November 2019
Available online 24 December 2019

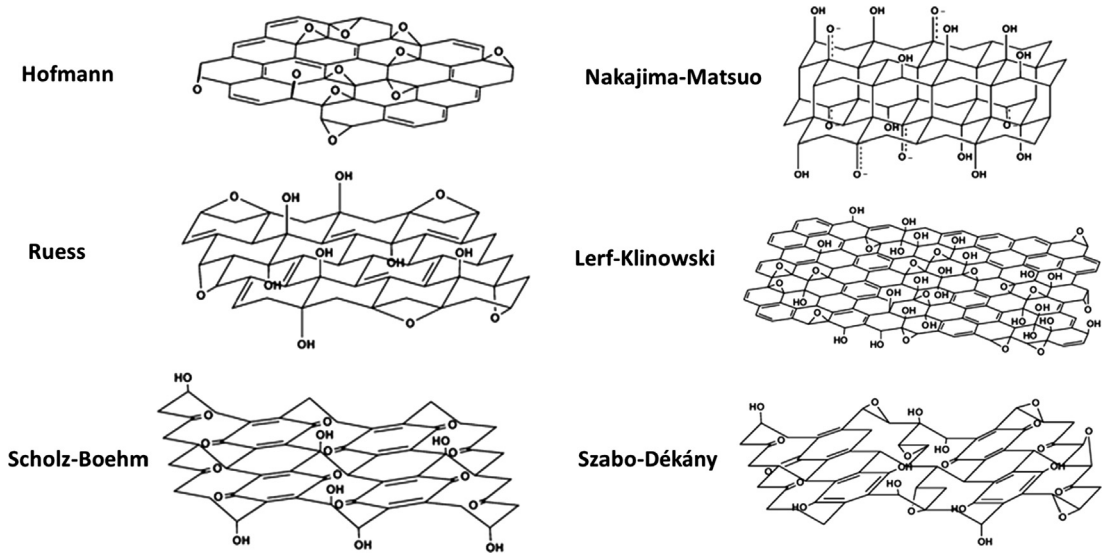

Fig. 1. Various models of the GO structure (Dreyer et al., 2010).

nanomaterials (CBNs) has been rapidly increasing. CBNs are among the most explored groups of nanostructures employed for adsorption applications (Alonso et al., 2017; Kumar et al., 2017; Sarma et al., 2019; Smith and Rodrigues 2015; Thines et al., 2017). CBNs (e.g., fullerene, carbon nanotubes (CNTs), and graphene) are most commonly used in environmental applications due to their physical and chemical properties, including their high electrical conductivity and good adsorption performance (Chabot et al., 2014). Among CBNs, graphene-based materials (GBMs), including graphene, graphene oxide (GO), reduced graphene oxide (rGO), and their composites with other potential nanomaterials (NMs), have been recognized as new generation adsorbents for the removal of organic compounds (e.g., nitrobenzene, organic dyes, bisphenol A, antibiotics, phenol, oil) (Kumar et al., 2018; Wang et al., 2013; Yan et al., 2015) and heavy metals (e.g., As, Pb, Hg) (Chandra et al., 2010; Cui et al., 2015).

To date, a number of reviews have been carried out to assess the adsorption capacities and related properties of graphene-based NMs and their composites in the environmental field, e.g., adsorptive removal of metal contaminants (Hiew et al., 2018; Perreault et al., 2015; Sherlala et al., 2018; Xu et al., 2018), adsorptive removal of dyes/pharmaceuticals (Hiew et al., 2018), adsorptive removal of organic structures (Chabot et al., 2014), and sensing of metal species/gaseous pollutants/organic molecules/microbes (Perreault et al., 2015; Samaddar et al., 2018). However, none of them have exclusively focused on the removal of VOCs. This review was hence organized to explore the basic knowledge on the applications of GBMs toward the adsorptive removal of VOCs. Furthermore, their performance was thoroughly evaluated against other materials, and the present limitations and future perspectives of GBM techniques are discussed. Additionally, the partition coefficient (PC) (derived from maximum adsorption capacitates) of covered GBMs was evaluated to assess their performance against VOC removal in a more practical sense to avoid biases associated with maximum adsorption capacities (Szulejko et al., 2019). A detailed discussion is also presented to describe the effect of functionality, physical/chemical structure of graphene and their composites, and their mechanism of VOC removal. In addition, the synthesis techniques favorable to design graphene-based adsorbents have also been described to upgrade their efficiency for VOC removal. This article offers valuable insights into the applicability of GBMs while improving the skills and strategies needed for designing and constructing efficient forms of GBMs for eliminating VOCs.

2. Potential of graphene-based materials as adsorbents for environmental remediation

In general, at least one dimension of NMs is confined to the nanometer scale (i.e., ~100 nm) (Gajewicz et al., 2012). Compared with non-nanoscale materials, NMs like GBMs possess superior physicochemical properties, such as mechanical, catalytic, optical, and electrical properties (Klaine et al., 2008). Graphene, which is the most recently developed material among CBNs, is organized as a 2D sheet of sp^2-hexagonal-bonded carbon atoms (Compton and Nguyen 2010; Kaatz and Bultheel 2013). In light of the relative difficulty and high cost required for graphene synthesis, much effort has been devoted to developing effective and inexpensive materials such as GO for mass production (Lotya et al., 2009; Yang et al., 2013). GO can further be reduced to rGO with the aid of reduction processes (Kumar et al., 2018; Pei and Cheng 2012). GO produced by the oxidation of graphite under acidic conditions is commonly used, as it provides several advantages over pristine graphene: (1) providing hydrophilic functional groups that enable chemical functionalization and dispersion in many matrices; (2) featuring wider physical properties than pure graphene due to structural heterogeneity; and (3) offering effective production cost and large-scale production of GBMs (Pei and Cheng 2012).

Gas adsorption by GBMs is primarily based on their intermolecular forces with the gaseous pollutants. The strength of the interaction is determined by specific surface area, surface properties (e.g., type of interaction forces and polarization potential), pore volume, and pore size distribution of the GBMs as adsorbents. The following discussion provides a detailed description of the surface characteristics of GBMs as adsorbents.

2.1. Structural characteristics of GO-based materials

The GBMs displayed excellent performances for the removal of VOCs, both as pure and composite structures. Among the covered graphene-based structures, GO and rGO have been used most intensively for applications toward VOC removal. Therefore, this section is mainly organized to describe the structural characteristics of GO. The Hummer's method has been explored most intensively for the preparation of GO (Marcano et al., 2010). (The synthesis process for the preparation of GO based on the Hummer's method is shown in Fig. 1S.) GO is usually treated as a single layer of graphite oxide. Although graphite oxide was first synthesized by Brodie in the mid-1800 s, its atomic/electronic structure remains relatively unknown (Chen et al.,

2012).

The various models of the GO structure are shown in Fig. 1 (Dreyer et al., 2010). Hofmann and Holst (1939) first suggested that graphite oxide features a simple structure in which the basal structure consists of epoxy group-modified planar carbon layers with a molecular formula of C_2O. Afterward, various proposals were put forward for the graphite oxide structure such as: (1) a wrinkled carbon sheet containing *trans*-linked cyclohexane chairs with oxygen-containing groups (Ruess 1947), (2) a corrugated carbon sheet replaced by carbonyl and hydroxyl from the epoxy and ether groups (Scholz and Boehm 1969), and (3) two carbon layers linked to each other by sp^3 C−C bonds with carbonyl and hydroxyl groups (Nakajima et al., 1988; Nakajima and Matsuo 1994). Lerf et al., (1998) suggested the graphite oxide structure in which unoxidized benzene rings (C═C) and a wrinkled region of alicyclic 6-membered ring ethers are distributed randomly in a flat aromatic region. Szabó et al., (2006) recently proposed a new model based on the carbon network consisting of the two types of regions: *trans*-linked cyclohexane chairs with functional groups (e.g., tertiary OH, ketone, and phenol) and flat hexagonal ribbon forms with C═C double bonds (Szabó et al., 2006). In case of rGO, the oxygen groups present on the surface of GO were reduced with the help of a reducing process, e.g., chemical and physical reduction processes. Such reduction is helpful in improving the graphitic nature in GO by reducing the defects generated through the incorporation of functional groups (Erickson et al., 2010).

2.2. Specific surface area

In general, the area of interaction with molecules increases with the increase in adsorbent surface area (Lizzio and DeBarr 1996). Hence, the adsorption capacity of a sorbent is considered proportional to its surface area. In comparison with conventional materials, the advantage of NMs on adsorption processes is their high porosity and specific surface area. Gaseous contaminants can be captured more efficiently with nano-scale voids. The specific surface area is defined as the surface area available for adsorption per mass of adsorbent. The theoretical specific surface area of completely exfoliated graphene is assumed to be 2620 m^2/m (Stankovich et al., 2007). However, the surface area of graphene calculated by several experimental techniques is rather less than the theoretical surface area of graphene.

As shown in Table 1, the surface area of the graphene material is higher in a composite structure than in the pristine form, e.g., GO and rGO. Among the covered materials, the composite of GO with MIL-101 exhibited the highest BET surface area of 3502.2 m^2/g (Sun et al., 2014), while the value for GO itself was 236.4 m^2/g (Yu et al., 2018). As such, the formation of a graphene composite with MOFs (e.g., MIL-101 (Zheng et al., 2018; Zhou et al., 2014), MOF-5 (Liu et al., 2015), Cu-BTC (Li et al., 2016; Yan et al., 2016), and ZIF-8 (Chu et al., 2018)) is especially helpful in improving its surface area. The reduction of GO to rGO also displayed a slight increase in BET surface area from 236.4 m^2/g to 292.9 m^2/g (Yu et al., 2018).

2.3. Surface characteristics

In general, the capacity of GBMs to adsorb VOCs can be substantially improved through surface modification. For instance, the modification of rGO with KOH enhanced its adsorption capacity from 0.8 to 1.23 mg/g for acetaldehyde (Kim et al., 2018). The polar VOCs usually prefer to interact with polar surfaces, e.g., surface of GO. Hence, GO can interact easily with the polar VOCs via polar functional groups present on its surface (Bao et al., 2016; Dreyer et al., 2010; Petit et al., 2009; Xu et al., 2012). On the other hand, pristine graphene prefers to interact with hydrophobic pollutants. Alternatively, in the case of rGO, its preference between polar and non-polar targets vary depending on the extent of reduction to which GO was subject. For instance, comparatively hydrophilic forms of GBMs (e.g., GO/MOF composites and activated rGO) were employed preferably for the removal of polar VOCs (e.g., alcoholic and carbonyl VOCs) (Kim et al., 2018; Liu et al., 2015; Yan et al., 2016; Zhou et al., 2014). However, the proper balance between hydrophobicity, surface area, and functionality is to be considered to design an efficient adsorbent for VOCs. Hence, the potential utility of GBMs is recognized for the efficient removal of VOCs.

3. Adsorption of VOCs on graphene-based materials

The adsorption capacity of GBMs has been explored for a variety of VOCs, such as aromatic, aliphatic, alcoholic, carbonyl, and chlorinated species. In this section, the adsorption parameters of different graphene-materials are discussed with respect to each type of important VOCs. The basic information on the synthesis methods employed for the preparation of graphene materials is discussed in supplementary material.)

3.1. Removal of aromatic VOCs

VOCs such as benzene, toluene, and xylene are the major representative components of aromatic VOCs. In general, these aromatic VOCs are preferably adsorbed on hydrophobic surfaces relative to hydrophilic surfaces (Chu et al., 2018; Yu et al., 2018). The potential of diverse graphene variants (e.g., GO, rGO, and their composites) have been explored for the adsorption-based removal of aromatic VOCs. Because of the presence of oxygen functionalities on the surface, GO is likely to exhibit comparatively low hydrophobicity (e.g., relative to rGO and pristine graphene). As a result, GO may exhibit less adsorption capacity for aromatic VOCs in comparison to its aforementioned counterparts. For instance, in the case of initial loading of 50 ppm benzene, GO and rGO were reported to have adsorption capacities of 216.2 and 276.4 mg/g, respectively, in a continuous flow reactor (Yu et al., 2018). Because of the hydrophobic nature and enhanced tendency to form π-π bonds, rGO can play a dominant role in increasing the adsorption capacity of aromatic VOCs relative to GO. In addition to hydrophobicity, it was also speculated that the better adsorptive performance of rGO was due to its higher surface area in comparison to GO. The surface areas for rGO and GO were found to be 292.6 and 236.4 m^2/g, respectively (Yu et al., 2018). Although the surface area and partial hydrophobic character of GO were prominent, their reported capacity values are suspected to be mistakenly overestimated. According to a numerical integration of their breakthrough data for GO, a capacity of only 1.1 mg/g was estimated instead of the reported value of 216 mg/g. (The benzene removal capacity of 1.1 mg/g was calculated for GO from the information provided in Yu et al. (2018): 100% breakthrough when loading 50 ppm benzene at flow rate: 40 cm^3/min (for 150 min).) Because of this questionable issue, the discussion on the performance data made by Yu et al. (2018) was confined only under limited conditions.

By considering the high surface area provided by the GBMs, GO was employed to improve the benzene adsorption capacities for OMC (Szczęśniak et al., 2018a). The incorporation of GO with OMC and KOH activation led to an increase in the surface area from 740 (for pristine OMC) to 1370 m^2/g. The increase in pore volume of OMC from 0.61 to 1.06 cm^3/g was also observed after the formation of the GO/OMC composite. Benzene adsorption capacities of 633 and 750 mg/g were observed for OMC and the GO/OMC composite, respectively, at 20 °C. The adsorption capacities of both the tested materials were found to increase at a lower temperature of −196 °C and pressure of 760 mm Hg. It was observed that at the aforementioned conditions, OMC and the GO/OMC composite were able to adsorb 632.7 and 750 mg/g benzene, respectively. It was postulated that the high surface area, pore volume, and increased π-π interactions were responsible for such enhancement (Szczęśniak et al., 2018a).

The activation of GO/OMC with KOH was also found to be important in improving its surface area by generating pores (especially smaller pores with size > 2 nm) in GO/OMC (Fig. 2) (Szczęśniak et al.,

Table 1
Performance of GBMs for the removal of different target VOCs.

S.No.	Type of graphene material	Synthesis methods	S_{BET} (m^2/g)	Target VOC	Adsorption capacity (given value)	Adsorption capacity (mg/g)	Temperature (K)	Pressure (Pa)	Partition coefficient (mol/kg/Pa) derived from maximum adsorption capacity	% removal of initial values/cycles	Ref.
Aromatic VOCs											
Benzene											
1	GO	Modified Hummers'	236.4	Benzene	216.2 mg/g	216.2	293.15	5.07	0.55*	NP	(Yu et al., 2018)
2	rGO	Modified Hummers'	292.6	Benzene	276.4 mg/g	276.4	293.15	5.07	0.70*	NP	(Yu et al., 2018)
3	GO/OMC	GO: Modified Hummers' and ultasonication GO/OMC: soft-templating method using resorcinol	1370	Benzene	9.6 mmol/g	749.9	293.15	10,018	0.00096	NP	(Szczęśniak et al., 2018a)
4	rGO/PPy	GO: modified Hummers' method Composite: one-step carbonization	2780	Benzene	15.8 mmol/g	1234.2	293.15	10,018	0.0016	NP	(Szczęśniak et al., 2018b)
5	GO/CNF	GO: Improved Hummers' method GO/CNF: Electrospinning	473	Benzene	83.2 cm^3/g	289.8	293.15	9829.4	0.00038	NP	(Guo et al., 2016)
6	GO/MOF-5	GO: Modified Hummers' method GO/MOF-5: solvothermal	439	Benzene	72 cm^3/g	250.8	303.15	9829.4	0.00021	NP	(Liu et al., 2015)
Toluene											
1	GO	Modified Hummers'	236.4	Toluene	240.6 mg/g	240.6	293.15	5.07	0.52*	NP	(Yu et al., 2018)
2	rGO	Modified Hummers'	292.6	Toluene	304.4 mg/g	304.4	293.15	5.07	0.65*	Almost unchanged/ 4	(Yu et al., 2018)
3	GP		54	Toluene	466 mm^3/g	1.9	293.15	3.042	0.0068	NP	(Kim et al., 2018)
4	rGOMW	GO: Hummers' method	326	Toluene	1710 mm^3/g	7	293.15	3.042	0.025	NP	(Kim et al., 2018)
5	rGOMWKOH	GO: Hummers' method	491	Toluene	3510 mm^3/g	14.4	293.15	3.042	0.051	NP	(Kim et al., 2018)
6	Cu-BTC@GO	GO: Hummers' method Cu-BTC@GO: mechanochemical	1362.7	Toluene	9.1 mmol/g	838.5	298			NP	(Li et al., 2016)
7	ZIF-8/GO	ZIF-8/GO: chemical synthesis	1112	Toluene	123 mg/g	123	303			87/5	(Chu et al., 2018)
Aliphatic VOCs											
1	MIL-101@GO	GO: Modified Hummers' method MIL-101@GO: Hydrothermal method	3502.2	N-hexane	1042.1 mg/g	1042.2	298		0.0042	96.8/5	(Sun et al., 2014)
Alcoholic VOCs											
1	GO/MOF-5	GO: Modified Hummers' method GO/MOF-5: solvothermal	727	Ethanol	77 cm^3/g	158.2	303.15	9808.75	0.00035	NP	(Liu et al., 2015)
2	Cu-BTC@GO	GO: Hummers' method Cu-BTC@GO: chemical synthesis	1459	Ethanol	13.6 mmol/g	635	303			NP	(Yan et al., 2016)
Carbonyl VOCs											
1	G-GND/S	GO: Modified Hummer's method GND: using photo-Fenton reactions G-GND/S: solvothermal		Formaldehyde	22.8 mg/g	22.8	293.15			NP	(Wu et al., 2015)

(*continued on next page*)

Table 1 (*continued*)

S.No.	Type of graphene material	Synthesis methods	S_{BET} (m^2/g)	Target VOC	Adsorption capacity (given value)	Adsorption capacity (mg/g)	Temperature (K)	Pressure (Pa)	Partition coefficient (mol/kg/Pa) derived from maximum adsorption capacity	% removal of initial values/cycles	Ref.
2	GN/E	CNTs: catalytic chemical vapor deposition method GO: Modified Hummers' method GN/E: Chemical reduction	252	Formaldehyde	27.43 mg/g	27.43	293.15			NP	(Wu et al., 2017)
3	GP		54	Acetaldehyde	165 mm^3/g	0.32	293.15	3.042	0.0024	NP	(Kim et al., 2018)
4	rGOMW	GO: Hummers' method	326	Acetaldehyde	405 mm^3/g	0.8	293.15	3.042	0.0060	NP	(Kim et al., 2018)
5	rGOMWKOH	GO: Hummers' method	491	Acetaldehyde	630 mm^3/g	1.23	293.15	3.042	0.0092	NP	(Kim et al., 2018)
6	GO/MIL-101	GO: Modified Hummers' method GO/MIL-101: hydrothermal method	2928	Acetone	20.10 mmol/g	1167.4	288	16,180	0.0012	91.5/6	(Zhou et al., 2014)
7	GO/CNF	GO: Improved Hummers' method GO/CNF: Electrospinning	473	Butanone	130.5 cm^3/g	419.6	293.15	9270.8	0.00063	NP	(Guo et al., 2016)
Chlorinated VOCs											
1	MIL-101/GO	MIL-101/GO: Hydrothermal synthesis	2026	CCl_4	2368.1 mg/g	2368.1	303			NP	(Zheng et al., 2018)
2	ZIF-8/GO	ZIF-8/GO: chemical synthesis		CH_2Cl_2	240 mg/g	240		48.672	0.058	NP	(Zhou et al., 2016)

Abbreviations: NP- not performed.

* Please refer to possible errors in the reported capacity values as discussed in Section 4.1.

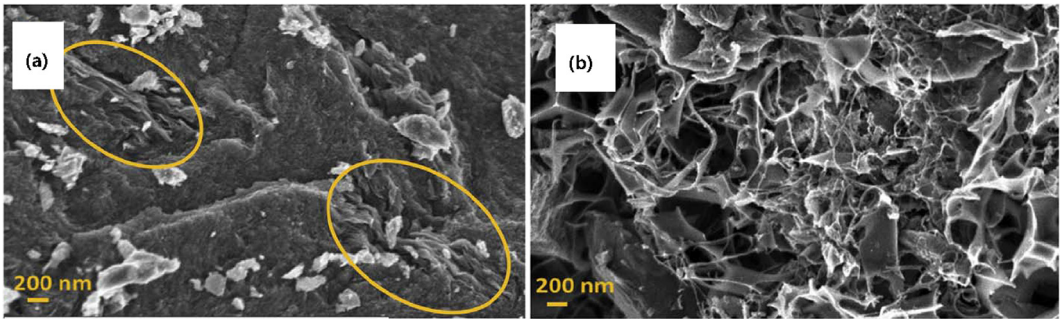

Fig. 2. SEM images of ordered mesoporous carbon/graphene oxide (GO/OMC) composite (a) before and (b) after KOH activation (Szczęśniak et al., 2018a). The KOH activation of the GO/OMC composites enhanced the porosity of the composite material.

2018a). The KOH-based activation of GO/OMC led to an increase in surface area from 690 m^2/g (without activation) to 1370 m^2/g (with activation). Likewise, KOH activation is also effective in improving the surface area of the PPy/rGO composite from 290 m^2/g to 2780 m^2/g (Szczęśniak et al., 2018b). The KOH activation of PPy/rGO led to the generation of mesopores (2–5 nm size), which was speculated as the main cause of the enhanced adsorption of benzene. The KOH activated PPy/rGO exhibited an adsorption capacity of 1234 mg/g at 20 °C and $p/p_0 \sim 1$. Likewise, the composite of GO with carbon composite nanofibers (CNFs) was able to adsorb 290 mg/g of benzene at 20 °C and a relative pressure of 0.98 (Guo et al., 2016). Under similar conditions, the GO/CNF composite outperformed activated carbon fibers (ACF); the ACF exhibited an adsorption volume of 255 mg/g for benzene at 20 °C and 0.98 relative pressure.

The composite of GO with MOF-5 was also reported to be efficient in the removal of benzene gas and exhibited a removal capacity of 251 mg/g (Liu et al., 2015). It was suspected that even with the high porosity of MOFs, they were not able to retain small molecules under ambient conditions due to the absence of strong and non-specific adsorption forces between small molecules and MOFs. The incorporation of graphene-based materials with MOFs solved the aforementioned problems of holding small molecules. In this regard, the GO/MOF-5 composite was prepared using varying proportions of GO, such as 1.75 wt%, 3.5 wt%, 5.25 wt%, and 7 wt%. Out of all these composites, the one prepared by using 5.25 wt% GO was the best performer in terms of benzene removal capacity with the highest surface area and pore volume among the tested ratios of GO and MOF-5 (Fig. 3). The use of 5.25% GO with MOF-5 increased the surface area of MOF-5 from 539 m^2/g to 727 m^2/g. Likewise, the pore volume of MOF-5 was also improved from 0.27 cm^3/g to 0.35 cm^3/g through the addition of 5.25% GO.

The GO and rGO have also been tested for the removal of toluene. The possibility of GO/rGO to show π–π bonds, hydrophobic interaction, and electrostatic interactions with toluene can be useful to show desirable adsorption of toluene on their surfaces. In a report, three types of GBMs (i.e., (1) graphene platelets (GP), (2) rGOMW, and (3) KOH activated rGOMW (rGOMWKOH)) were tested for toluene adsorption, and their performances were compared with AC (Kim et al., 2018). (Note that the AC employed in this case is usually used as a commercial adsorption filter for air conditioners.) These graphene-based materials followed the order GP (2 mg/g) < rGOMW (7 mg/g) < rGOMWKOH (14.4 mg/g) for the removal of toluene. As shown in Table 1, the specific surface area of the aforementioned materials also followed the same trend. It was suspected that the possibility of making π-π interactions (e.g., between the aromatic ring of toluene and π-electron rich region of graphene materials) with toluene and the specific surface area of these materials was the major reason for the adsorption of toluene molecules. However, as per the toluene adsorption capacity with respect to the specific surface area, GP exhibited the maximum affinity towards toluene. The ratio of toluene adsorption volume and specific surface area was found to be 7.17, 2.13, and 1.78 mm^3/m^2 for GP, rGOMW, and rGOMWKOH, respectively. It was postulated that the higher graphitic character of GP was responsible for the higher adsorption to specific surface area ratio. In contrast, the level of defects in graphene increased through the treatment of MW and KOH due to the generation of functional groups. However, as mentioned above, rGOMWKOH was the best performer in terms of maximum adsorption capacity for toluene removal due to a higher specific surface area. Moreover, the rGOMWKOH displayed almost similar adsorptive performance compared to AC for toluene removal (Fig. 4). It is also worth mentioning that the amount of rGOMWKOH was 0.5 g, while similar

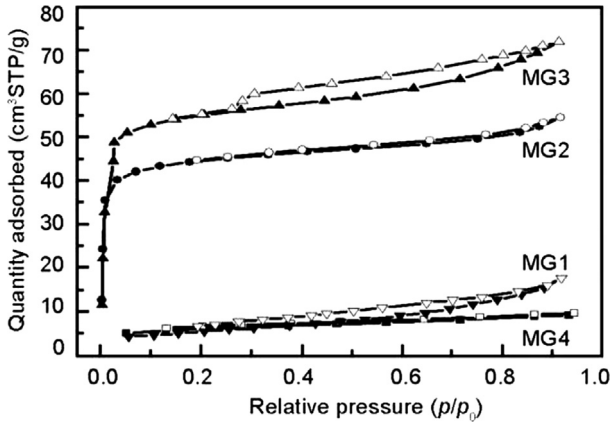

Fig. 3. Adsorption-desorption isotherms for graphene oxide/metal organic framework-5 (GO/MOF-5) for benzene (Liu et al., 2015). MG (1–4) represents GO/MOF-5 composite with 1.75%, 3.5%, 5.25%, and 7% of GO in MOF-5.

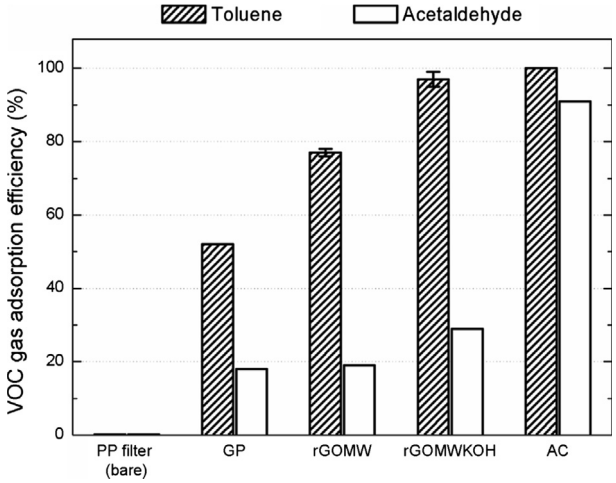

Fig. 4. Comparison of toluene and acetaldehyde removal capacity between rGOMWKOH and other adsorbents (Kim et al., 2018).

toluene uptake was achieved by 1.25 g of AC.

The combination of GO with MOFs (e.g., Cu-BTC and ZIF-8) was also reported to improve the removal capacity of toluene (Chu et al., 2018; Li et al., 2016). The addition of GO in MOFs usually displayed enhanced adsorption for aromatic analytes by providing π-electrons for the interaction. In contrast, MOFs generally exhibit high specific surface area, which is of immense importance to achieve high adsorption of analytes. However, in many cases, especially for Cu-BTC, the adsorptive performances of these structures were degraded under humid conditions (Li et al., 2016). In such cases, in addition to improving the adsorption efficiency for aromatic molecules, the use of graphene materials with MOFs is highly beneficial, as it can improve the aqueous stability of MOFs.

In this regard, the composite of GO and Cu-BTC was prepared using a mechanochemical method; this composite exhibited improved surface area and total pore volume of 1362.7 m^2/g and 0.87 cm^3/g, respectively, when compared to pristine Cu-BTC with a surface area of 1188.3 m^2/g and a pore volume of 0.77 cm^3/g (Li et al., 2016). Moreover, with these enhanced characteristics, GO/Cu-BTC displayed an adsorption capacity of 839 mg/g, which was 47% higher than that of Cu-BTC (Fig. 5). The composite of ZIF-8 and GO displayed a nominal decrease in the adsorption capacity for toluene, when the performance was tested under high humidity conditions (Chu et al., 2018). The toluene adsorption capacity observed for ZIF-8/GO at 10%, 55%, and 80% relative humidity (RH) was 123 mg/g, 116 mg/g, 110 mg/g, respectively. In contrast, the toluene adsorption values for ZIF-8 (97 mg/g), although tested at 55% RH, was far larger.

Overall, graphene-based materials are an excellent platform for improving the adsorptive removal of aromatic VOCs. These structures provided not only higher surface area, but also π-electrons to interact with aromatic VOCs. Moreover, the graphene-based structures are also excellent in improving the adsorptive parameters of several other structures, e.g., polymers and coordination polymers.

3.2. Removal of aliphatic and alcoholic VOCs

The release of aliphatic VOCs, especially n-hexane, into the environment occurs very frequently (Sun et al., 2014). n-hexane is generally used in the shoe, bag, electronic, food, oil extraction, and chemical industries. The adsorption of n-hexane is usually considered a safe, fast, and economical method for its mitigation. The use of a GO/MIL-101 composite was found to be a good option to remove n-hexane from air (Sun et al., 2014). The GO/MIL-101 composite exhibited a maximum n-hexane adsorption capacity of 1042.1 mg/g. Formation of the composite with GO led to 93% enhancement in the adsorption capacity of MIL-101 (i.e., 540.3 mg/g). It was assumed that the GO-derived increase in the surface area and dispersive forces in the composite material were responsible for the enhanced n-hexane adsorption. Moreover, the n-hexane adsorption capacity of this graphene-MOF-based composite was maintained at 96.8%, even after five subsequent adsorption-desorption cycles. The authors claimed that the performance of the GO/MIL-101 composite was superior compared to AC and zeolite Y (Sun et al., 2014). Despite the superior performance of graphene-based composites for n-hexane removal, limited studies have been conducted in this area of research.

In case of alcoholic VOCs, adsorptive removal of ethanol is mainly explored using graphene materials. However, in a few instances, successful simulation studies have been performed to check the feasibility of other alcoholic VOCs, e.g., methanol, for adsorption on the graphene surface (Esrafili and Dinparast 2018). In contrast, GBMs were majorly employed as a composite with MOFs for the adsorption of ethanol (Liu et al., 2015; Yan et al., 2016). In general, graphene materials have been reported to improve the surface area and forces/interactions with small molecules, e.g., ethanol, in the form of a composite, which are critical for high ethanol adsorption. For instance, the high surface area, porous structure, and availability of oxygen functionality led to the 158.2 mg/g adsorption of ethanol. In another report, the adsorption capacity of 635 mg/g for ethanol was achieved by a Cu-BTC/GO composite at 303 K (Yan et al., 2016). (Note that in this study, the ethanol adsorption characteristics of Cu-BTC/GO was tested for a refrigeration application.)

3.3. Removal of carbonyl VOCs

Aldehydes and ketones are the major carbonyl VOCs affecting the environment. GBMs have also been used efficiently for the removal of carbonyl VOCs. In a report on the removal of indoor formaldehyde, diverse forms of graphene-based materials were employed, e.g., an amino functionalized graphene sponge (G/S) and amino functionalized graphene sponge decorated with graphene nanodots (G-GND/S) (Wu et al., 2015). G-GND/S is characterized by a high concentration of amine groups on its surface in comparison to G/S, which led to its high interaction with formaldehyde molecules (Fig. 6). Consequently, G-GND/S exhibited a higher adsorption capacity (22.8 mg/g) for formaldehyde removal compared to G/S (~7.5 mg/g).

In another report, an amino-functionalized graphene aerogel was used in its pristine form and as a composite with CNTs for the removal of gaseous formaldehyde (Wu et al., 2017). The adsorption of

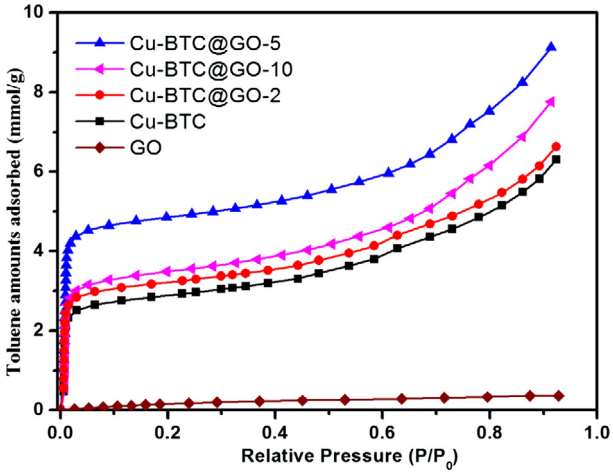

Fig. 5. Adsorption isotherms for toluene on GO, Cu-BTC and their composites (Li et al., 2016).

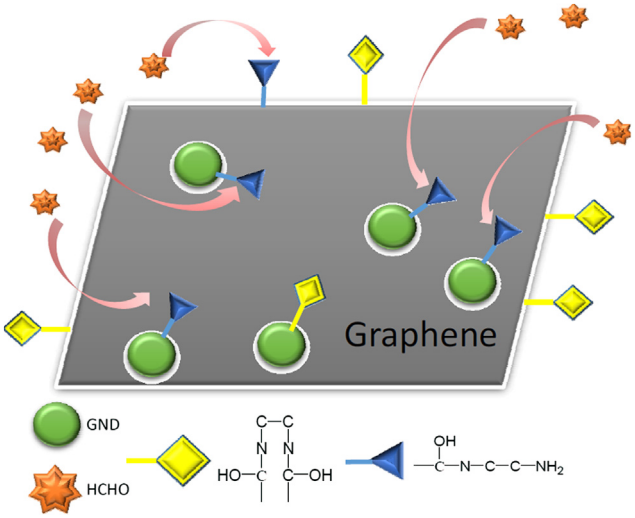

Fig. 6. Interaction of amino graphene nanodots decorated functionalized graphene sponge with formaldehyde molecules (Wu et al., 2015).

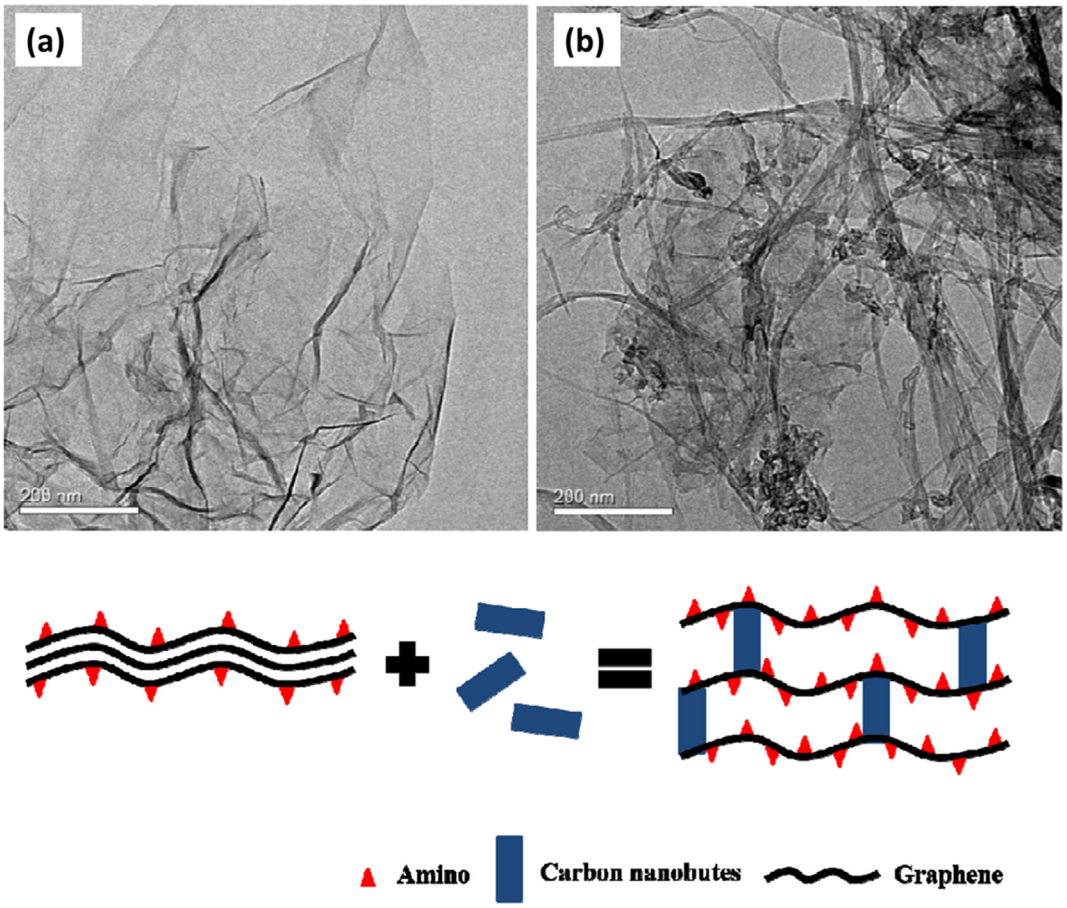

Fig. 7. TEM images and possible stacking pattern of graphene aerogels and CNT-modified graphene aerogels (Wu et al., 2017). (a) TEM image of graphene aerogel, (b) TEM image of CNT-modified graphene aerogel, and (c) stacking of CNTs between layers of graphene, which led to the exposure of more amino groups for the chemical adsorption of formaldehyde.

formaldehyde on the aforementioned amino-functionalized graphene materials was mediated by chemical and physical adsorption processes. The chemical adsorption process mainly occurred between the van der Waals forces through amino groups and the carbonyl group of formaldehyde. In the case of the CNT-modified amino-functionalized graphene aerogel (GN/E), CNTs provided support to graphene layers to reduce the pore diameter. As shown in Fig. 7, the use of CNTs with graphene-based aerogels led to the exposure of more amino functionalities for the uptake of formaldehyde. Likewise, the favorable (e.g., favorable for formaldehyde uptake) pore size enhanced the physical capturing of formaldehyde molecules. GN/E exhibited an adsorption capacity of 27.4 mg/g for formaldehyde.

In another report, three types of graphene materials ((1) GP, (2) rGOMW, and (3) rGOMWKOH) were employed to remove gaseous acetaldehyde (Kim et al., 2018). Microwave and KOH treatment caused enhancement in the acetaldehyde uptake efficiency of the graphene-based materials. The acetaldehyde uptake capacity of GP, rGOMW, and rGOMWKOH were observed as 0.32 mg/g, 0.8 mg/g, and 1.24 mg/g, respectively. As shown in Table 1 and Section 4.1, these materials were also tested for the removal of toluene. Accordingly, they displayed higher adsorption capacities for toluene (in comparison with acetaldehyde), indicating that they have high affinity for non-polar molecules. Moreover, rGOMWKOH was unable to adsorb acetaldehyde below 20 ppmv. (Note that the acetaldehyde adsorption experiments were performed at 30 ppmv acetaldehyde concentration.) The rGOMWKOH exhibited 30% removal efficiency for gaseous acetaldehyde.

In addition to aldehydes, the adsorptive performance of graphene-based materials has also been explored against ketonic VOCs, e.g., acetone and butanone (Guo et al., 2016; Zhou et al., 2014). In a typical study, GO was demonstrated to enhance the adsorption capabilities of MIL-101 for acetone removal by 44% (Zhou et al., 2014). The GO/MIL-101 composite exhibited an acetone adsorption capacity of 1167 mg/g at 288 K and 161.8 mbar inlet concentration. The strong interactions between composite materials and acetone were estimated by measuring acetone desorption activation energy. The desorption activation energy values for GO/MIL-101 and MIL-101 were calculated as 62.68 kJ/mol and 48.01 kJ/mol, respectively. This composite is also efficient for multiple cycles of adsorption–desorption for acetone. The composite maintained 91.3% of its initial adsorption capacity after six cycles (Fig. 8). (Note that the desorption experiment was performed at 0.04 mbar acetone pressure.) In the case of butanone, the mesoporous fibrous structures prepared using GO and PAN displayed an adsorption capacity of 420 mg/g at 20 °C and 0.98 relative pressure (Guo et al., 2016). Interestingly, the use of GO with PAN enhanced the mesoporous character and surface oxygen content of the resulting material. Moreover, the GO/PAN composite favored the adsorption of non-polar VOCs in comparison to polar VOCs, e.g., benzene. These authors also claimed that the performance of GO/PAN composite was better than AC nanofibers for butanone adsorption.

3.4. Removal of chlorinated VOCs

The GBMs are also effective in the removal of chlorinated VOCs, e.g., carbon tetrachloride and methylene chloride (Zheng et al., 2018; Zhou et al., 2016). The composite of graphene materials with MOFs is found to be promising for the adsorptive removal of chlorinated VOCs. For instance, the incorporation of GO in a MIL-101 (Cr) MOF/GO

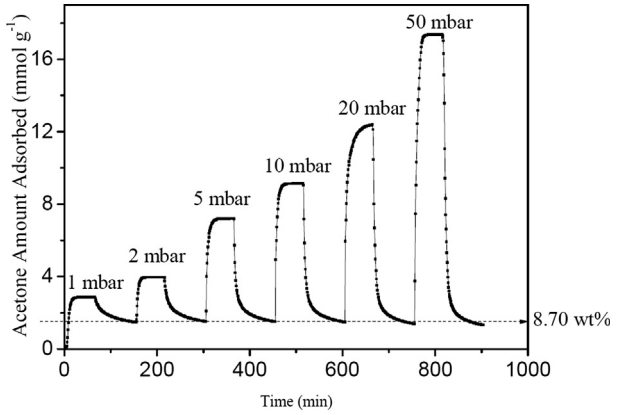

Fig. 8. Adsorption-desorption cycles for acetone on a graphene oxide- MIL-101 (GO/MIL-101) composite at 298 K (Zhou et al., 2014).

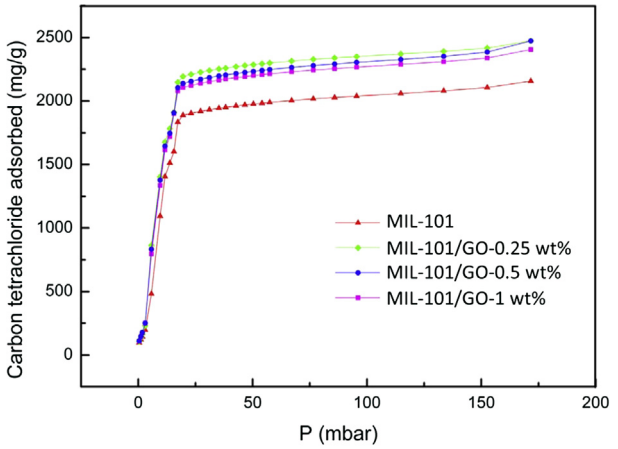

Fig. 9. Adsorption isotherm for carbon tetrachloride on MIL-101 and MIL-101 composites with 0.25 wt%, 0.5 wt%, and 1 wt% GO (Zheng et al., 2018). MIL101/GO-0.25 wt% was the best performer for the adsorption of carbon tetrachloride among the tested samples.

composite enhanced the CCl_4 adsorption capacity from 2044 mg/g to 2368 mg/g (Zheng et al., 2018). An increase of 16% was observed in the CCl_4 adsorption capacity of MIL-101 (Cr) after the addition of GO. Different combinations of MIL-101 (Cr) and GO were also tested to achieve optimum adsorption capacity for CCl_4 by employing different amounts of GO, e.g., 0.25 wt%, 0.5 wt%, 1 wt%, and 2 wt%. As shown in Fig. 9, the MIL-101 (Cr) with 0.25 wt% of GO was the best performer for CCl_4 removal. It was suggested that several factors were responsible for improving the performance of GO/MIL-101 towards CCl_4 removal, such as (1) increased surface area: the surface area of MIL-101 was increased from 1832 m^2/g to 2026 m^2/g after incorporation of 0.25 wt % GO in MIL-101; (2) increased dispersive forces: the GO tends to increase dispersive forces on the composite surface, which are very helpful in holding small molecules; and (3) the generation of more defects: the presence of more defects on the composite surface (in comparison to MIL-101) facilitates the adsorption of carbon tetrachloride molecules; all while (4) forming new pores: the coordination of GO functional groups with unsaturated metal sites of MOFs led to the formation of new pores, which are again helpful in the uptake of carbon tetrachloride (Zheng et al., 2018). Moreover, these authors also claimed that the MIL-101/GO-0.25 wt% composite exhibited considerably enhanced adsorption performance over most commonly explored conventional adsorbents (e.g., MCM-11, activated carbon, and zeolite Y) by 2.2, 3.9, and 5.5 times, respectively. Thus, the excellence of graphene-based adsorbents is supported (in terms of adsorption capacity for CCl_4) relative to conventional adsorbents. Likewise, the synergistic effect between GO and ZIF-8 was considered for the higher adsorption of CH_2Cl_2 on a ZIF-8/GO composite, when compared with ZIF-8 alone (Zhou et al., 2016). The ZIF-8/GO displayed a much higher adsorption capacity (e.g., 240 mg/g) for CH_2Cl_2, while micro-scale and nano-scale ZIF-8 exhibited adsorption capacities of 69 mg/g and 138 mg/g, respectively.

On the basis of type of VOCs, different types GBMs were found to be best performers in terms of maximum adsorption capacity. For instance, for the adsorption of benzene, PPy/rGO was found to be most superior GBM with 1234.2 mg/g adsorption capacity (Szczęśniak et al., 2018b). The excellent performance of PPy/rGO composite was ascribed to its high surface area of 2780 m^2/g along with the presence of mesopores. Likewise, composite of Cu-BTC and GO was one of the best GBM performers for toluene (in terms of maximum adsorption capacity: 838.5 mg/g) (Li et al., 2016). In case of carbonyl and chlorinated VOCs, composite of GO with MIL-101 was the most suitable option for acetone and carbon tetra chloride with the maximum adsorption capacity values of 1283.6 and 2368.1 mg/g, respectively (Zheng et al., 2018; Zhou et al., 2014).

Overall, the use of graphene materials alone and in combination with other potent structures demonstrated excellent potential in the removal of diverse VOCs. In several studies, it was claimed that these GBMs are much better than the conventional adsorbents, e.g., AC and zeolites. However, the performance of the adsorbent material may be altered significantly with experimental conditions, such as high/low partial pressures of the target gas (Szulejko et al., 2019). Interestingly, certain adsorbents show excellent performance in controlled conditions (e.g., setting of initial partial pressure of target gas at an unrealistically high level). However, such materials can perform very poorly in more practical situations where the concentration of the target pollutant is not as high as the experimental conditions. To avoid such challenges, the use of proper metrics (such as partition coefficient (PC)) is important to assess the performance of adsorbents by reducing the source of bias in such considerations (Ridha and Webley 2009; Szulejko et al., 2019). In the next section, we calculate the PC of the covered materials to compare their performance among different materials.

4. Performance evaluation

An assessment of the adsorption processes is performed considering the adsorption capacities and PC measurements. A high PC value implies that the adsorption capacity of gaseous analytes increases, owing to the high affinity of gases for adsorbents (Ridha and Webley 2009). Adsorption at the gas–solid interface can change depending on the temperature, pressure, initial pressure of the target gas, surface characteristics, and presence or absence of water and oxygen. The variations in these experimental parameters can alter the adsorption capacity of the adsorbents against the target VOCs. In most of the surveyed studies, the adsorption capacities were assessed at different experimental conditions (e.g., initial loading conditions), which makes it difficult to directly compare the performances between different adsorbents.

As per Henry's law, at a low pressure of the target gas and at high temperature conditions, the gas adsorption is linearly dependent upon its pressure (Ridha and Webley 2009). It was proposed that at a lower pressure of the target gas, the interaction between target gas molecules was negligible, while the adsorption of the gas was only due to interaction of the target gas molecules and adsorbent surface. In almost all studies carried out to assess the removal capacity of GBMs, the concept of PC was not considered or calculated. Herein, we extracted data from the provided information in cited articles to calculate the PC (mol/kg/Pa) values between different adsorbents. However, in a few cases, due to lack of adequate information, it was not possible to determine the PC values. In such situations, the PC data are left blank in Table 1.

In the case of benzene, the maximum adsorption capacity reported for activated PPy/rGO was 1234.2 mg/g, which was highest in terms of the reported adsorption capacity (when compared with covered GBMs)

(Szczęśniak et al., 2018b). It is worth mentioning that this adsorption performance was obtained at a benzene saturation vapor pressure at 20 °C (i.e., 10.018 kPa). PPy/rGO was also the best performer among GBMs in terms of PC values. The calculated PC for PPy/rGO was 0.0016 mol/kg/Pa. (Note that the PC values mentioned in Table 1 for GO and rGO (i.e., Yu et al. (2018)) were not considered for performance evaluation due to of the possible error as aforementioned.) Guo et al., (2016) compared the benzene removal performances of ACF and ACNF (derived from PAN) with their graphene composite, i.e., GO/CNF. It was observed that the PC value (mol/kg/Pa) of GO/CNF (0.00038) was slightly better in both maximum adsorption capacity and PC values, when compared to ACF (0.00033) and ACNF (0.00036) (Table 1). Interestingly, as reviewed by Szulejko et al., (2019), a few ACs were seen to perform better than GBMs for the removal of benzene at zero/low partial pressure conditions.

Kim et al., (2018) compared the performance of AC with rGOMWKOH by taking the initial toluene concentration as 30 ppmv. Accordingly, it was found that 0.5 g of rGOMWKOH displayed 98% of the toluene adsorption of 1.25 g AC. The calculated PC for rGOMWKOH was 0.051 mol/kg/Pa, which was best among the considered studies listed in Table 1. (Note that due to unavailability of the exact toluene adsorption capacity for AC, we are unable to calculate PC for AC.) The superiority (in terms of maximum adsorption capacity) of GBMs for VOCs over other adsorbents are described in Section 4. The performance comparison for the removal of other VOCs is shown in Table 1. Note that due to unavailability of sufficient data, we are unable to calculate PC for a few materials, e.g., Cu-BTC@GO, ZIF-8/GO, G-GND/S, GN/E, and MIL-101/GO (Table 1).

The regeneration and reusability of any adsorbent are critical variables in determining its operational cost and viability for practical use. A very few attempts have been performed to determine the reusability/regenerability of GBMs for VOCs removal. As shown in Table 1, only 4 GBMs have been tested for repeated adsorption-desorption cycles. These adsorbents were mainly regenerated via either of three methods: (1) thermal treatment, (2) solvent treatment followed by thermal treatment, and (3) low pressure treatment. The rGO regenerated by thermal treatment showcased almost insignificant changes in adsorption capacity for toluene after four consecutive cycles (Yu et al., 2018), although the absolute magnitude of adsorption capacity reported by these authors needs to be re-estimated as discussed above. In terms of regeneration, the MIL-101@GO was found excellent with 96.8% recovery (by low pressure (0.07 mbar) treatment) in adsorption capacity for n-hexane after five consecutive cycles (Fig. 10a) (Sun et al., 2014). Likewise, aforementioned composite structure maintained 91.5% of adsorption capacity for acetone after six regeneration cycles through low pressure treatment (e.g., 0.04 mbar) (Fig. 10b) (Zhou et al., 2014).

5. Conclusion and future perspectives

The consistent release of VOCs in the environment has increased the focus of researchers for the development of adsorbents for their removal. The quick and timely removal of these harmful molecules is necessary to avoid their exposure to living beings. A variety of conventional and advanced structures have been employed to remove VOCs from the environment. Among them, GBMs (e.g., GO, rGO, and their composites with other structures) displayed great potential in the removal of diverse VOCs.

To understand the applicability of GBMs as efficient adsorbent for VOCs, this article surveyed the performances of GBMs for the removal of diverse VOCs, such as aromatic, aliphatic, alcoholic, carbonyl, and chlorinated VOCs. In addition, we also covered synthesis approaches to prepare GBMs and the importance of their properties (e.g., surface area and surface/structural characteristics) as adsorbents for gaseous targets, especially VOCs. In the majority of the studies, VOC adsorption parameters were estimated at different experimental conditions. Moreover, the capacity of graphene-based adsorbents was assessed at unrealistically high initial pressures. These limited conditions restricted us from making a direct comparison between different adsorbents. Thus, the performance of GBMs towards VOC removal under real life conditions has been estimated through the calculation of PC using maximum adsorption capacities. In terms of maximum adsorption capacity, the composite forms of graphene materials are found to be superior. Likewise, if the capacity is compared in terms of PC, the composite forms and activated non-composite (e.g., rGOMWKOH) forms of graphene materials are found to be more effective for almost all type of VOCs, especially for aromatic and carbonyl VOCs. Overall, graphene-based materials generally displayed promising potentials for the removal of VOCs. The graphene-material-based nanotechnological approaches can thus be applied as next-generation air purification technology, especially for the removal of VOCs. However, a few associated challenges should be resolved before their implementation in air purification systems.

The toxicity of used GBMs should be the prime concern, as they are small enough to be inhaled and/or absorbed into the body. Thus, GBMs can deleteriously affect human health due to their physical and chemical characteristics (e.g., size, shape, form, cohesion, aggregation, and disaggregation). In addition, the range of their potential adverse effects on the environment is uncertain. The possible harmful effects of GBMs as VOC adsorbents should be identified, studied, and rectified before their implementation as commercial adsorbents for VOCs. In addition, the fate of adsorbed VOCs should also be studied.

As mentioned earlier, the performances of GBMs were commonly tested under non-realistically arbitrary conditions. The performances of these GBMs should be evaluated under real-life conditions to judge

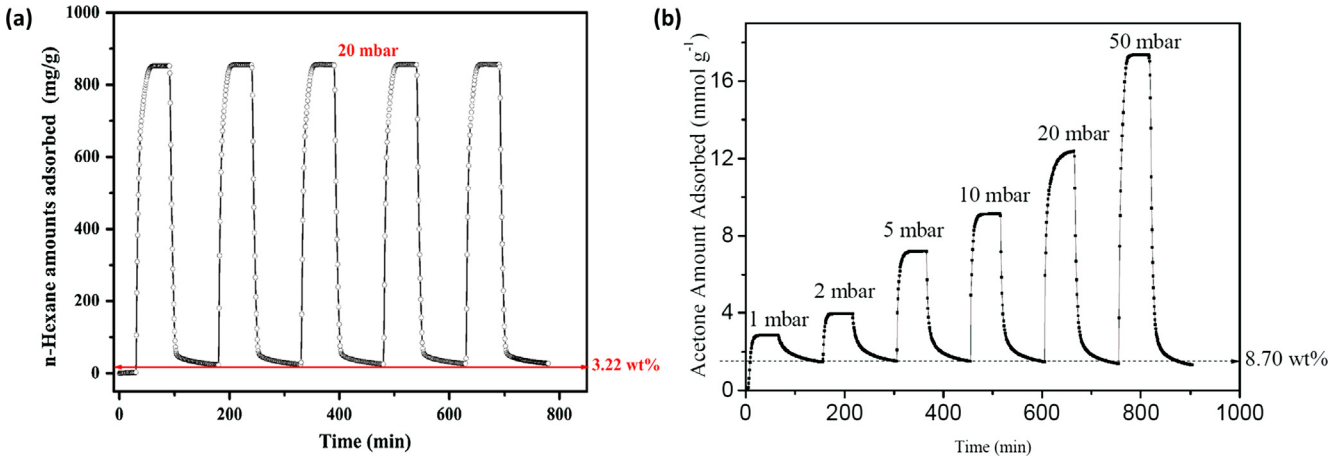

Fig. 10. Consecutive cycles of adsorption-desorption for (a) n-hexane (Sun et al., 2014) and (b) acetone (Zhou et al., 2014) on GO/MIL-101 composite.

their applicability in a more practical sense. Moreover, a reusable adsorbent is always beneficial for both commercial and customer aspects. Researchers should try to prepare reusable adsorbents for VOCs with a special focus on the fate of the adsorbed VOCs. In addition, the regeneration process should be easy to reproduce, even within homes. Accordingly, the adsorbent for VOCs should be designed by considering the regeneration and disposal of the adsorbed material. The life of the adsorbent is a main concern while purchasing an air purifier. The life and recycle period should also be studied before implementation of GBMs as adsorbents for VOCs. The cost of graphene is another concern for GBMs for such applications. However, in the future, large-scale production of GBMs may exert a considerable impact on increasing their merits in pricewise respects as well.

Acknowledgements

This research acknowledges the support made by a grant from the National Research Foundation of Korea (NRF) funded by the Ministry of Science, ICT & Future Planning (Grant No: 2016R1E1A1A01940995). We sincerely acknowledge and thank Prof. Jan E Szulejko for critically reviewing our ms and pointing out errors in some cited articles along with supporting evidence and data sets.

Appendix A. Supplementary material

Supplementary data to this article can be found online at https://doi.org/10.1016/j.envint.2019.105356.

References

Alonso, A., Moral-Vico, J., Abo Markeb, A., Busquets-Fité, M., Komilis, D., Puntes, V., Sánchez, A., Font, X., 2017. Critical review of existing nanomaterial adsorbents to capture carbon dioxide and methane. Sci. Total Environ. 595, 51–62. https://doi.org/10.1016/j.scitotenv.2017.03.229.

Bao, C., Bi, S., Zhang, H., Zhao, J., Wang, P., Yue, C.Y., Yang, J., 2016. Graphene oxide beads for fast clean-up of hazardous chemicals. J. Mater. Chem. A 4, 9437–9446.

Belaissaoui, B., Le Moullec, Y., Favre, E., 2016. Energy efficiency of a hybrid membrane/condensation process for VOC (Volatile Organic Compounds) recovery from air: A generic approach. Energy 95, 291–302. https://doi.org/10.1016/j.energy.2015.12.006.

Brunekreef, B., Holgate, S.T., 2002. Air pollution and health. Lancet 360, 1233–1242.

Campesi, M.A., Luzi, C.D., Barreto, G.F., Martínez, O.M., 2015. Evaluation of an adsorption system to concentrate VOC in air streams prior to catalytic incineration. J. Environ. Manage. 154, 216–224. https://doi.org/10.1016/j.jenvman.2015.02.028.

Chabot, V., Higgins, D., Yu, A., Xiao, X., Chen, Z., Zhang, J., 2014. A review of graphene and graphene oxide sponge: material synthesis and applications to energy and the environment. Energy Environ. Sci. 7, 1564–1596.

Chandra, V., Park, J., Chun, Y., Lee, J.W., Hwang, I.C., Kim, K.S., 2010. Water-dispersible magnetite-reduced graphene oxide composites for arsenic removal. ACS Nano 4, 3979–3986. https://doi.org/10.1021/nn1008897.

Chen, D., Feng, H., Li, J., 2012. Graphene oxide: preparation, functionalization, and electrochemical applications. Chem. Rev. 112, 6027–6053. https://doi.org/10.1021/cr300115g.

Cheng, J., Li, L., Li, Y., Wang, Q., He, C., 2019. Fabrication of pillar[5]arene-polymer-functionalized cotton fibers as adsorbents for adsorption of organic pollutants in water and volatile organic compounds in air. Cellulose 26, 3299–3312. https://doi.org/10.1007/s10570-019-02315-1.

Cheng, Z., Lu, L., Kennes, C., Yu, J., Chen, J., 2016. Treatment of gaseous toluene in three biofilters inoculated with fungi/bacteria: Microbial analysis, performance and starvation response. J. Hazard. Mater. 303, 83–93. https://doi.org/10.1016/j.jhazmat.2015.10.017.

Chu, F., Zheng, Y., Wen, B., Zhou, L., Yan, J., Chen, Y., 2018. Adsorption of toluene with water on zeolitic imidazolate framework-8/graphene oxide hybrid nanocomposites in a humid atmosphere. RSC Adv. 8, 2426–2432. https://doi.org/10.1039/C7RA12931A.

Compton, O.C., Nguyen, S.T., 2010. Graphene oxide, highly reduced graphene oxide, and graphene: versatile building blocks for carbon-based materials. Small 6, 711–723. https://doi.org/10.1002/smll.200901934.

Cui, L.M., Wang, Y.G., Gao, L., Hu, L.H., Yan, L.G., Wei, Q., Du, B., 2015. EDTA functionalized magnetic graphene oxide for removal of Pb(II), Hg(II) and Cu(II) in water treatment: adsorption mechanism and separation property. Chem. Eng. J. 281, 1–10. https://doi.org/10.1016/j.cej.2015.06.043.

DeCoste, J.B., Peterson, G.W., 2014. Metal-organic frameworks for air purification of toxic chemicals. Chem. Rev. 114, 5695–5727. https://doi.org/10.1021/cr4006473.

Dreyer, D.R., Park, S., Bielawski, C.W., Ruoff, R.S., 2010. The chemistry of graphene oxide. Chem. Soc. Rev. 39, 228–240. https://doi.org/10.1039/B917103G.

Erickson, K., Erni, R., Lee, Z., Alem, N., Gannett, W., Zettl, A., 2010. Determination of the local chemical structure of graphene oxide and reduced graphene oxide. Adv. Mater. 22, 4467–4472. https://doi.org/10.1002/adma.201000732.

Esrafili, M.D., Dinparast, L., 2018. The selective adsorption of formaldehyde and methanol over Al- or Si-decorated graphene oxide: a DFT study. J. Mol. Graph. Model. 80, 25–31. https://doi.org/10.1016/j.jmgm.2017.12.025.

Gajewicz, A., Rasulev, B., Dinadayalane, T.C., Urbaszek, P., Puzyn, T., Leszczynska, D., Leszczynski, J., 2012. Advancing risk assessment of engineered nanomaterials: application of computational approaches. Adv. Drug Deliv. Rev. 64, 1663–1693. https://doi.org/10.1016/j.addr.2012.05.014.

Guo, Z., Huang, J., Xue, Z., Wang, X., 2016. Electrospun graphene oxide/carbon composite nanofibers with well-developed mesoporous structure and their adsorption performance for benzene and butanone. Chem. Eng. J. 306, 99–106. https://doi.org/10.1016/j.cej.2016.07.048.

Hiew, B.Y.Z., Lee, L.Y., Lee, X.J., Thangalazhy-Gopakumar, S., Gan, S., Lim, S.S., Pan, G.-T., Yang, T.C.-K., Chiu, W.S., Khiew, P.S., 2018. Review on synthesis of 3D graphene-based configurations and their adsorption performance for hazardous water pollutants. Process Saf. Environ. Prot. 116, 262–286. https://doi.org/10.1016/j.psep.2018.02.010.

Hu, S.-C., Chen, Y.-C., Lin, X.-Z., Shiue, A., Huang, P.-H., Chen, Y.-C., Chang, S.-M., Tseng, C.-H., Zhou, B., 2018. Characterization and adsorption capacity of potassium permanganate used to modify activated carbon filter media for indoor formaldehyde removal. Environ. Sci. Pollut. Res. 25, 28525–28545. https://doi.org/10.1007/s11356-018-2681-z.

Kaatz, F.H., Bultheel, A., 2013. Statistical properties of carbon nanostructures. J. Math. Chem. 51, 1211–1220.

Kamal, M.S., Razzak, S.A., Hossain, M.M., 2016. Catalytic oxidation of volatile organic compounds (VOCs) – A review. Atmos. Environ. 140, 117–134. https://doi.org/10.1016/j.atmosenv.2016.05.031.

Kampa, M., Castanas, E., 2008. Human health effects of air pollution. Environ. Pollut. 151, 362–367. https://doi.org/10.1016/j.envpol.2007.06.012.

Kim, J.M., Kim, J.H., Lee, C.Y., Jerng, D.W., Ahn, H.S., 2018. Toluene and acetaldehyde removal from air on to graphene-based adsorbents with microsized pores. J. Hazard. Mater. 344, 458–465. https://doi.org/10.1016/j.jhazmat.2017.10.038.

Klaine, S.J., Alvarez, P.J.J., Batley, G.E., Fernandes, T.F., Handy, R.D., Lyon, D.Y., Mahendra, S., McLaughlin, M.J., Lead, J.R., 2008. Nanomaterials in the environment: behavior, fate, bioavailability, and effects. Environ. Toxicol. Chem. 27, 1825–1851. https://doi.org/10.1897/08-090.1.

Kumar, V., Kim, K.-H., Park, J.-W., Hong, J., Kumar, S., 2017. Graphene and its nanocomposites as a platform for environmental applications. Chem. Eng. J. 315, 210–232. https://doi.org/10.1016/j.cej.2017.01.008.

Kumar, V., Kumar, P., Pournara, A., Vellingiri, K., Kim, K.-H., 2018. Nanomaterials for the sensing of narcotics: challenges and opportunities. TrAC. Trends Anal. Chem. 106, 84–115. https://doi.org/10.1016/j.trac.2018.07.003.

Kumar, V., Kumar, S., Kim, K.-H., Tsang, D.C.W., Lee, S.-S., 2019. Metal organic frameworks as potent treatment media for odorants and volatiles in air. Environ. Res. 168, 336–356. https://doi.org/10.1016/j.envres.2018.10.002.

Lerf, A., He, H., Forster, M., Klinowski, J., 1998. Structure of Graphite Oxide Revisited. J. Phys. Chem. B 102, 4477–4482. https://doi.org/10.1021/jp9731821.

Li, J., Li, M., Zhang, J., Ye, D., Zhu, X., Liao, Q., 2013. A microbial fuel cell capable of converting gaseous toluene to electricity. Biochem. Eng. J. 75, 39–46. https://doi.org/10.1016/j.bej.2013.03.015.

Li, Y., Miao, J., Sun, X., Xiao, J., Li, Y., Wang, H., Xia, Q., Li, Z., 2016. Mechanochemical synthesis of Cu-BTC@GO with enhanced water stability and toluene adsorption capacity. Chem. Eng. J. 298, 191–197. https://doi.org/10.1016/j.cej.2016.03.141.

Likens, G.E., Bormann, F.H., 1974. Acid rain: a serious regional environmental problem. Science 184, 1176–1179.

Likens, G.E., Driscoll, C.T., Buso, D.C., 1996. Long-term effects of acid rain: response and recovery of a forest ecosystem. Science 272, 244–246.

Liu, G.-Q., Wan, M.-X., Huang, Z.-H., Kang, F.-Y., 2015. Preparation of graphene/metal-organic composites and their adsorption performance for benzene and ethanol. New Carbon Mater. 30, 566–571. https://doi.org/10.1016/S1872-5805(15)60205-0.

Lizzio, A.A., DeBarr, J.A., 1996. Effect of surface area and chemisorbed oxygen on the SO2 adsorption capacity of activated char. Fuel 75, 1515–1522.

Lotya, M., Hernandez, Y., King, P.J., Smith, R.J., Nicolosi, V., Karlsson, L.S., Blighe, F.M., De, S., Wang, Z., McGovern, I., 2009. Liquid phase production of graphene by exfoliation of graphite in surfactant/water solutions. J. Am. Chem. Soc. 131, 3611–3620.

Mao, M., Li, Y., Hou, J., Zeng, M., Zhao, X., 2015. Extremely efficient full solar spectrum light driven thermocatalytic activity for the oxidation of VOCs on OMS-2 nanorod catalyst. Appl. Catal. B 174–175, 496–503. https://doi.org/10.1016/j.apcatb.2015.03.044.

Marcano, D.C., Kosynkin, D.V., Berlin, J.M., Sinitskii, A., Sun, Z., Slesarev, A., Alemany, L.B., Lu, W., Tour, J.M., 2010. Improved Synthesis of Graphene Oxide. Acs Nano 4, 4806–4814. https://doi.org/10.1021/nn1006368.

Minitha, C.R., Lalitha, M., Jeyachandran, Y.L., Senthilkumar, L., Kumar, R.T.R., 2017. Adsorption behaviour of reduced graphene oxide towards cationic and anionic dyes: Co-action of electrostatic and pi - pi interactions. Mater. Chem. Phys. 194, 243–252. https://doi.org/10.1016/j.matchemphys.2017.03.048.

Mishra, M., 2019. Poison in the air: Declining air quality in India. Lung India 36, 160–161. https://doi.org/10.4103/lungindia.lungindia_17_18.

Monzón, A., Guerrero, M.A.-J., 2004. Valuation of social and health effects of transport-related air pollution in Madrid (Spain). Sci. Total Environ. 334, 427–434.

Nakajima, T., Mabuchi, A., Hagiwara, R., 1988. A new structure model of graphite oxide. Carbon 26, 357–361. https://doi.org/10.1016/0008-6223(88)90227-8.

Nakajima, T., Matsuo, Y., 1994. Formation process and structure of graphite oxide.

Carbon 32, 469–475. https://doi.org/10.1016/0008-6223(94)90168-6.
Pei, S., Cheng, H.-M., 2012. The reduction of graphene oxide. Carbon 50, 3210–3228. https://doi.org/10.1016/j.carbon.2011.11.010.
Perreault, F., de Faria, A.F., Elimelech, M., 2015. Environmental applications of graphene-based nanomaterials. Chem. Soc. Rev. 44, 5861–5896. https://doi.org/10.1039/c5cs00021a.
Petit, C., Seredych, M., Bandosz, T.J., 2009. Revisiting the chemistry of graphite oxides and its effect on ammonia adsorption. J. Mater. Chem. 19, 9176–9185.
Ridha, F.N., Webley, P.A., 2009. Anomalous Henry's law behavior of nitrogen and carbon dioxide adsorption on alkali-exchanged chabazite zeolites. Sep. Purif. Technol. 67, 336–343.
Ruess, G., 1947. Über das Graphitoxyhydroxyd (Graphitoxyd). Monatshe. Chem. Verwandte Teile Wissenschaft. 76, 381–417. https://doi.org/10.1007/bf00898987.
Samaddar, P., Son, Y.-S., Tsang, D.C.W., Kim, K.-H., Kumar, S., 2018. Progress in graphene-based materials as superior media for sensing, sorption, and separation of gaseous pollutants. Coord. Chem. Rev. 368, 93–114. https://doi.org/10.1016/j.ccr.2018.04.013.
Sarma, G.K., Sen Gupta, S., Bhattacharyya, K.G., 2019. Nanomaterials as versatile adsorbents for heavy metal ions in water: a review. Environ. Sci. Pollut. Res. 26, 6245–6278. https://doi.org/10.1007/s11356-018-04093-y.
Scholz, W., Boehm, H., 1969. Untersuchungen am graphitoxid. VI. Betrachtungen zur struktur des graphitoxids. Zeitschrift Anorganische Allgemeine Chem. 369, 327–340.
Sherlala, A.I.A., Raman, A.A.A., Bello, M.M., Asghar, A., 2018. A review of the applications of organo-functionalized magnetic graphene oxide nanocomposites for heavy metal adsorption. Chemosphere 193, 1004–1017. https://doi.org/10.1016/j.chemosphere.2017.11.093.
Smith, S.C., Rodrigues, D.F., 2015. Carbon-based nanomaterials for removal of chemical and biological contaminants from water: A review of mechanisms and applications. Carbon 91, 122–143. https://doi.org/10.1016/j.carbon.2015.04.043.
Stankovich, S., Dikin, D.A., Piner, R.D., Kohlhaas, K.A., Kleinhammes, A., Jia, Y., Wu, Y., Nguyen, S.T., Ruoff, R.S., 2007. Synthesis of graphene-based nanosheets via chemical reduction of exfoliated graphite oxide. Carbon 45, 1558–1565. https://doi.org/10.1016/j.carbon.2007.02.034.
Sun, X., Xia, Q., Zhao, Z., Li, Y., Li, Z., 2014. Synthesis and adsorption performance of MIL-101(Cr)/graphite oxide composites with high capacities of n-hexane. Chem. Eng. J. 239, 226–232. https://doi.org/10.1016/j.cej.2013.11.024.
Szabó, T., Berkesi, O., Forgó, P., Josepovits, K., Sanakis, Y., Petridis, D., Dékány, I., 2006. Evolution of surface functional groups in a series of progressively oxidized graphite oxides. Chem. Mater. 18, 2740–2749.
Szczęśniak, B., Choma, J., Jaroniec, M., 2018a. Effect of graphene oxide on the adsorption properties of ordered mesoporous carbons toward H2, C6H6, CH4 and CO2. Micropor. Mesopor. Mater. 261, 105–110. https://doi.org/10.1016/j.micromeso.2017.10.054.
Szczęśniak, B., Osuchowski, Ł., Choma, J., Jaroniec, M., 2018b. Highly porous carbons obtained by activation of polypyrrole/reduced graphene oxide as effective adsorbents for CO2, H2 and C6H6. J. Porous Mater. 25, 621–627. https://doi.org/10.1007/s10934-017-0475-1.
Szulejko, J.E., Kim, K.-H., Parise, J., 2019. Seeking the most powerful and practical real-world sorbents for gaseous benzene as a representative volatile organic compound based on performance metrics. Sep. Purif. Technol. 212, 980–985. https://doi.org/10.1016/j.seppur.2018.11.001.
Thines, R.K., Mubarak, N.M., Nizamuddin, S., Sahu, J.N., Abdullah, E.C., Ganesan, P., 2017. Application potential of carbon nanomaterials in water and wastewater treatment: a review. J. Taiwan Inst. Chem. Eng. 72, 116–133. https://doi.org/10.1016/j.jtice.2017.01.018.
Veerapandian, S.K.P., Geyter, D.N., Giraudon, J.M., Lamonier, J.F., Morent, R., 2019. The use of zeolites for VOCs abatement by combining non-thermal plasma, adsorption, and/or catalysis: a review. Catalysts 9, 98.
Wang, H., Yang, W., Tian, P., Zhou, J., Tang, R., Wu, S., 2017. A highly active and anti-coking Pd-Pt/SiO2 catalyst for catalytic combustion of toluene at low temperature. Appl. Catal A 529, 60–67. https://doi.org/10.1016/j.apcata.2016.10.016.
Wang, S.B., Sun, H.Q., Ang, H.M., Tade, M.O., 2013. Adsorptive remediation of environmental pollutants using novel graphene-based nanomaterials. Chem. Eng. J. 226, 336–347. https://doi.org/10.1016/j.cej.2013.04.070.
Wu, L., Qin, Z., Zhang, L., Meng, T., Yu, F., Ma, J., 2017. CNT-enhanced amino-functionalized graphene aerogel adsorbent for highly efficient removal of formaldehyde. New J. Chem. 41, 2527–2533. https://doi.org/10.1039/C6NJ03643K.
Wu, L., Zhang, L., Meng, T., Yu, F., Chen, J., Ma, J., 2015. Facile synthesis of 3D amino-functional graphene-sponge composites decorated by graphene nanodots with enhanced removal of indoor formaldehyde. Aerosol Air Qual. Res. 15, 1028–1034.
Xu, J., Cao, Z., Zhang, Y., Yuan, Z., Lou, Z., Xu, X., Wang, X., 2018. A review of functionalized carbon nanotubes and graphene for heavy metal adsorption from water: Preparation, application, and mechanism. Chemosphere 195, 351–364. https://doi.org/10.1016/j.chemosphere.2017.12.061.
Xu, J., Liu, J., Wu, S., Yang, Q.-H., Wang, P., 2012. Graphene oxide mode-locked femtosecond erbium-doped fiber lasers. Opt. Express 20, 15474–15480.
Yan, H., Wu, H., Li, K., Wang, Y.W., Tao, X., Yang, H., Li, A.M., Cheng, R.S., 2015. Influence of the Surface Structure of Graphene Oxide on the Adsorption of Aromatic Organic Compounds from Water. ACS Appl. Mater. Interfaces 7, 6690–6697. https://doi.org/10.1021/acsami.5b00053.
Yan, J., Yu, Y., Xiao, J., Li, Y., Li, Z., 2016. Improved Ethanol Adsorption Capacity and Coefficient of Performance for Adsorption Chillers of Cu-BTC@GO Composite Prepared by Rapid Room Temperature Synthesis. Ind. Eng. Chem. Res. 55, 11767–11774. https://doi.org/10.1021/acs.iecr.6b03139.
Yang, H., Hernandez, Y., Schlierf, A., Felten, A., Eckmann, A., Johal, S., Louette, P., Pireaux, J.-J., Feng, X., Mullen, K., 2013. A simple method for graphene production based on exfoliation of graphite in water using 1-pyrenesulfonic acid sodium salt. Carbon 53, 357–365.
Yu, L., Wang, L., Xu, W., Chen, L., Fu, M., Wu, J., Ye, D., 2018. Adsorption of VOCs on reduced graphene oxide. J. Environ. Sci. 67, 171–178. https://doi.org/10.1016/j.jes.2017.08.022.
Zheng, Y., Chu, F., Zhang, B., Yan, J., Chen, Y., 2018. Ultrahigh adsorption capacities of carbon tetrachloride on MIL-101 and MIL-101/graphene oxide composites. Micropor. Mesopor. Mater. 263, 71–76. https://doi.org/10.1016/j.micromeso.2017.12.007.
Zhou, X., Huang, W., Shi, J., Zhao, Z., Xia, Q., Li, Y., Wang, H., Li, Z., 2014. A novel MOF/graphene oxide composite GrO@MIL-101 with high adsorption capacity for acetone. J. Mater. Chem. A 2, 4722–4730. https://doi.org/10.1039/C3TA15086K.
Zhou, Y., Zhou, L., Zhang, X., Chen, Y., 2016. Preparation of zeolitic imidazolate framework-8 /graphene oxide composites with enhanced VOCs adsorption capacity. Micropor. Mesopor. Mater. 225, 488–493. https://doi.org/10.1016/j.micromeso.2016.01.047.